



Trabecular bone density distribution in the scapula of patients undergoing reverse shoulder arthroplasty

Joshua H. Ehrlich, BHSc^a, Valeria Vendries, MSc^a, Timothy J. Bryant, PhD^{a,b},
Michael J. Rainbow, PhD^{a,b}, Heidi L. Ploeg, PhD^{a,b}, Ryan T. Bicknell, MD, MSc, FRCSC^{a,b,c,*}

^aHuman Mobility Research Centre, Queen's University, Kingston, ON, Canada

^bDepartment of Mechanical and Materials Engineering, Queen's University, Kingston, ON, Canada

^cDivision of Orthopaedic Surgery, Department of Surgery, Kingston General Hospital, Kingston, ON, Canada

ARTICLE INFO

Keywords:

Scapula
Bone density
Reverse shoulder arthroplasty
Glenoid

Level of evidence: Anatomy Study; Imaging

Background: To improve implant survival after reverse shoulder arthroplasty (RSA), surgeons need to maximize screw fixation. However, bone density variation and distribution within the scapula are not well understood as they relate to RSA. The three columns of bone in the scapula surrounding the glenoid fossa are the lateral border, the base of the coracoid process, and the spine of the scapula. In our previous study by Daalder et al on cadaveric specimens, the coracoid column was significantly less dense than the lateral border and spine. This study's objective was to verify whether these results are consistent with computer tomography (CT) scan information from patients undergoing RSA.

Methods: Two-dimensional axial CT images from twelve patients were segmented, and a three-dimensional digital model of the scapula was subsequently created using Mimics 17.0 Materialise Software (Leuven, Belgium). Hounsfield unit (HU) values representing cortical bone were filtered out to determine the distributions of trabecular bone density. An analysis of variance with post hoc Bonferroni tests determined the differences in bone density between the columns of bone in the scapula.

Results: The coracoid superolateral (270 ± 45.6 HU) to the suprascapular notch was significantly less dense than the inferior (356 ± 63.6 HU, $P = .03$, $d_s = 1.54$) and anterosuperior portion of the lateral border (353 ± 68.9 HU, $P = .04$, $d_s = 1.42$) and the posterior (368 ± 70 HU, $P = .007$, $d_s = 1.65$) and anterior spine (370 ± 78.9 HU, $P = .006$, $d_s = 1.54$).

Discussion/Conclusion: The higher-density bone in the spine and lateral border compared with the coracoid region may provide better bone purchase for screws when fixing the glenoid baseplate in RSA. This is in agreement with our previous study and indicates that the previous cadaveric results are applicable to clinical CT scan data. When these studies are taken together, they provide robust evidence for clinical applications, including having surgeons aim screws for higher-density regions to increase screw fixation, which may decrease micromotion and improve implant longevity.

© 2021 The Authors. Published by Elsevier Inc. on behalf of American Shoulder and Elbow Surgeons. This is an open access article under the CC BY-NC-ND license (<http://creativecommons.org/licenses/by-nc-nd/4.0/>).

Reverse shoulder arthroplasty (RSA) is an effective procedure for a variety of indications, including arthritis, a deficient rotator cuff, or failed prior shoulder prostheses.^{4,7,10,11,17,18,23} The most common need for revision surgery after RSA is due to glenoid component loosening.^{10,12,14,20} Improving long-term implant success and

reducing glenoid failure can be achieved with optimal screw placement.²²

Previous research has investigated the effects of screw positioning on glenoid baseplate fixation and simultaneously taken scapular morphology into account.^{7,8,11,16–18} This research indicates that surgeons should strive for far cortical fixation, maximum screw length, and placing screws in the best available bone when performing RSA.^{6,8,10,17,18,23} To do this intraoperatively, surgeons need information about scapular morphology and bone density. However, there is little investigation into targeting optimal screw placement while taking density into account.^{11,23}

Many studies have attempted to characterize the bony anatomy of the scapula, yet few have quantitatively analyzed bone density to guide ideal screw placement in RSA.^{3,5,10,21,28} Three columns of

The Queen's University Health Sciences and Affiliated Teaching Hospitals Research Ethics Board (HSREB) approved this study (TRAQ no. 6006038, Department Code: SURG-232-11 2020MAY06).

*Corresponding author: Ryan T. Bicknell, MD, MSc, FRCSC(C), Kingston Health Sciences Centre Kingston General Hospital Site, Watkins 3 76 Stuart Street, Kingston, ON, Canada K7L 2V7.

E-mail address: rtbickne@yahoo.ca (R.T. Bicknell).

<https://doi.org/10.1016/j.jseint.2021.09.004>

2666-6383/© 2021 The Authors. Published by Elsevier Inc. on behalf of American Shoulder and Elbow Surgeons. This is an open access article under the CC BY-NC-ND license (<http://creativecommons.org/licenses/by-nc-nd/4.0/>).

bone extend from the glenoid base, including the scapular spine, lateral border, and base of the coracoid process.^{10,17,19,23} These regions are traditionally thought to be the optimal location for screw placement.¹⁰ We question whether considering variation in bone density in the scapula will ultimately provide optimal targets for RSA screw placement.

Our previous study used a cadaver model to quantify the relative anatomic distribution of trabecular bone density in the three columns of the scapula adjacent to the glenoid accessible to screw fixation in RSA surgery.⁹ We found that the lateral border and spine had relatively denser trabecular bone than the base of the coracoid process, but there was no difference in overall bone density within these anatomic structures. When performing computed tomography (CT) scans in a clinical setting, scan parameters, including voltage and voxel spacing, are different compared with cadaveric studies, which are often carried out with increased voltage and decreased spacing. Therefore, it is important to perform the cadaveric methodology on patient scans to determine whether these results can be applied to actual clinical studies. Uncovering this information will prove to be valuable to guide future research and hypotheses.

The purpose of this study was to quantify the distribution of bone density in the scapulae of patients undergoing RSA to guide optimal screw placement and to compare these results with those found in our previous cadaveric study. To achieve this aim, we compared CT bone density in the three columns of the scapula around the glenoid that are targeted for screw placement.

We hypothesized that the *in vivo* results to be similar to the *in vitro* results found by Daalder et al. Accordingly, we believe the scapula's lateral border and spine contain denser bone than the base of the coracoid process and that there would be no differences in trabecular bone density within each anatomical structure.

Materials and methods

This study followed the methodology described by Daalder et al. However, this study analyzed CT data obtained from patients undergoing RSA surgery instead of cadaver specimens. Therefore, CT image acquisition was different as it met clinical standards.

Patient and image acquisition

The study included twelve patient scapulae, five women and seven men, with a mean age of 74 years (range, 54–83). The scapulae were CT scanned using a Toshiba Aquilion ONE CT Scanner (Toshiba, Nasu, Japan) with a voltage of 120 kVp and tube current of 350 mAs. Axial reconstructions were performed with a hard (FC35) convolutional kernel with 3.00-mm slice thickness, pixel size of 0.43 mm, and voxel size of (2 × 2 × 2) millimeters.³ In our previous study, scapulae were scanned with a tube current of 120 kVp and 100 mAs, 1.250-mm slice thickness, and voxel size of (0.625 × 0.625 × 0.625) millimeters.^{3,9}

Image processing

We analyzed the CT volumes using methods developed in our previous work.⁹ Briefly, Digital Imaging and Communications in Medicine (DICOM; National Electric Manufacturers Association, Rosslyn, VA, USA) image files of the scanned patient scapulae were imported into Mimics 17.0 software (Materialise Software, Leuven, Belgium) for segmentation. We generated three-dimensional (3D) tessellated surface mesh models and masks of the scapulae that contained 3D voxel locations with corresponding Hounsfield units (HUs). All left scapulae were mathematically mirrored to right scapulae to facilitate the analysis.²⁷

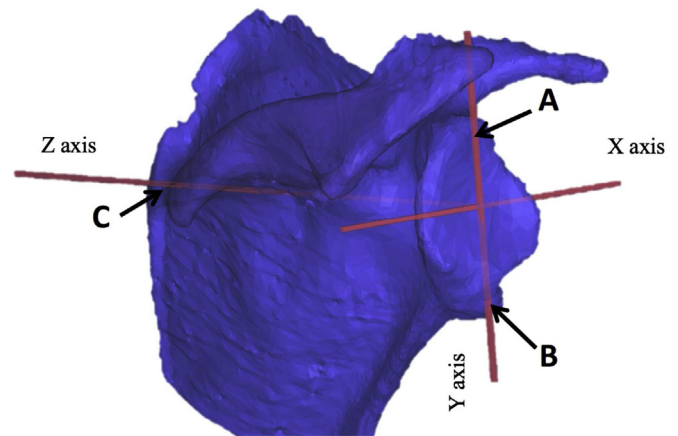


Figure 1 Quadripod oriented with respect to supraglenoid tubercle (A), infraglenoid tubercle (B), and triglonium spinae (C) in Mimics software (Materialise Software, Leuven, Belgium). The 3 points on the quadripod define the origin of the coordinate system (near the Middle of the glenoid surface), a point along the X axis (anterior to posterior), and a point along the Y axis (superior to inferior). The Z axis passes medial to lateral through the triglonium spinae.

The trabecular and cortical bone of the scanned scapulae were isolated from other tissues by segmentation of CT numbers above 0 HU. The scapula segmentation masks were then filled to ensure all bone material was included. To increase model accuracy, the segmented specimen masks and 3D models were visually inspected for any errors and supplemented by manual segments until the proper anatomic representation of the specimens was achieved.

A previously defined anatomical coordinate system was used to facilitate comparison across specimens and align the 3D surface mesh models and corresponding voxels. This also allowed comparison with our previous publication (Fig. 1).^{9,23} The coordinate system was based on a computer-assisted designed quadripod which was manually aligned to points on the supraglenoid and infraglenoid tubercles and the triglonium spinae. Each axis was aligned by different anatomical landmarks. The Y-axis (superior-inferior) was defined by the line connecting the supraglenoid and infraglenoid tubercles; the Z-axis (medial-lateral) was defined by the line connecting the triglonium spinae to the center of the glenoid, and the X-axis (anterior-posterior) was defined as the axis orthogonal to the Y-Z plane.

Regions of interest (ROIs) within each scapula were first defined and then extracted for analysis across specimens of the trabecular bone. Each ROI was determined based on its potential RSA glenoid baseplate screw position. ROIs include the base of the coracoid inferior to the suprascapular notch, the base of the coracoid lateral to the suprascapular notch, an anterior and posterior portion of the scapular spine, an anterosuperior portion of the lateral border, and an inferior portion of the lateral border. Each of the ROIs was visually determined on the surface mesh of each scapula displayed in MATLAB 9.4 R2018a (MathWorks, Natick, MA, USA). The ROIs were defined based on X, Y, and Z coordinates, and the corresponding voxels were extracted from the segmentation masks and subsequently registered to the surface model to check for accuracy (Figs. 2–7).⁹

Outcome measures

HU values were filtered to remove cortical bone: all voxels with HU values of 0 to 650 were kept, whereas all other HU values in the file were removed from the pool of data. HU values above 650 were

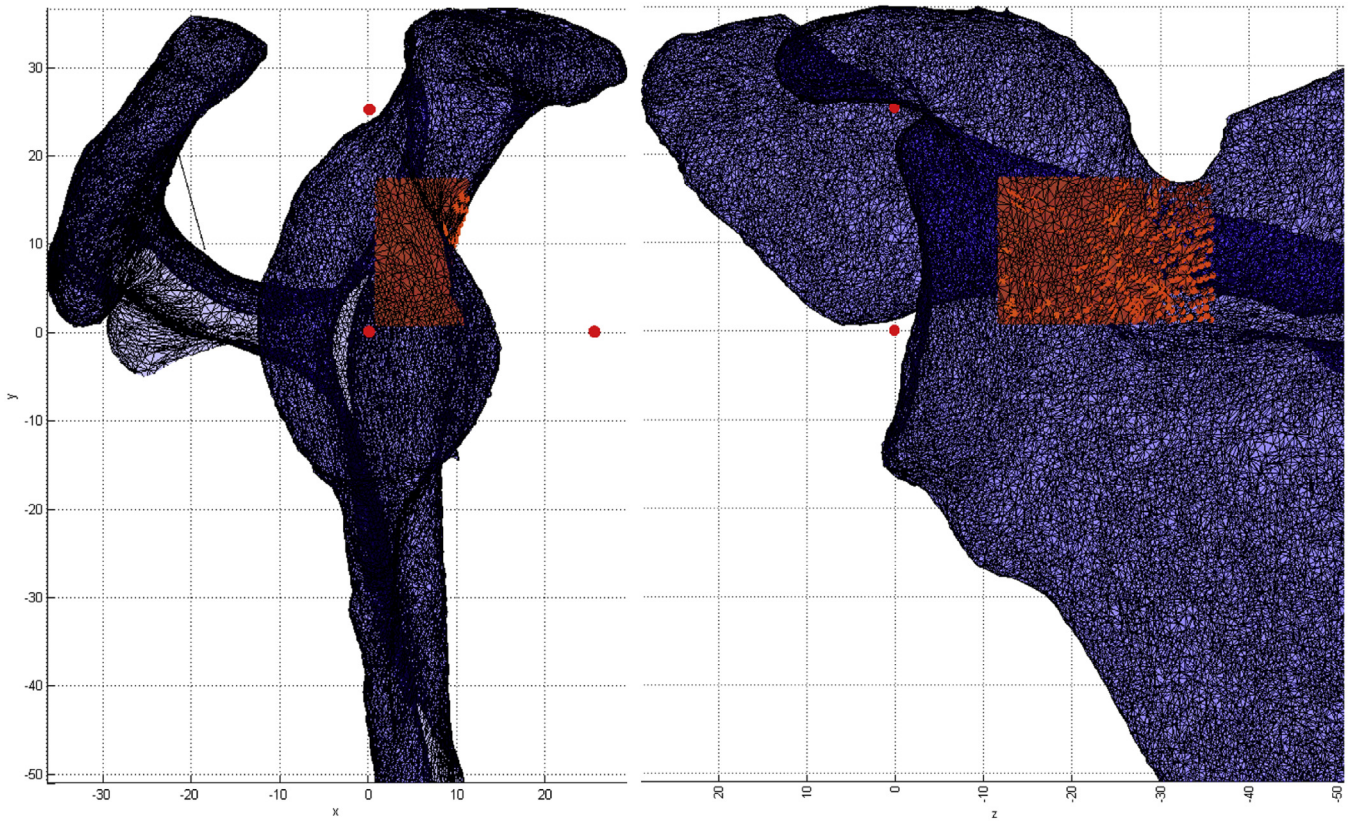


Figure 2 ROI in the inferior coracoid region inferior to the suprascapular notch, as shown in the sagittal lane (Left) and coronal plane (Right). The 3 red dots represent the P1, P2, and P3 coordinate points from the assigned quadrupod. ROI, region of interest.

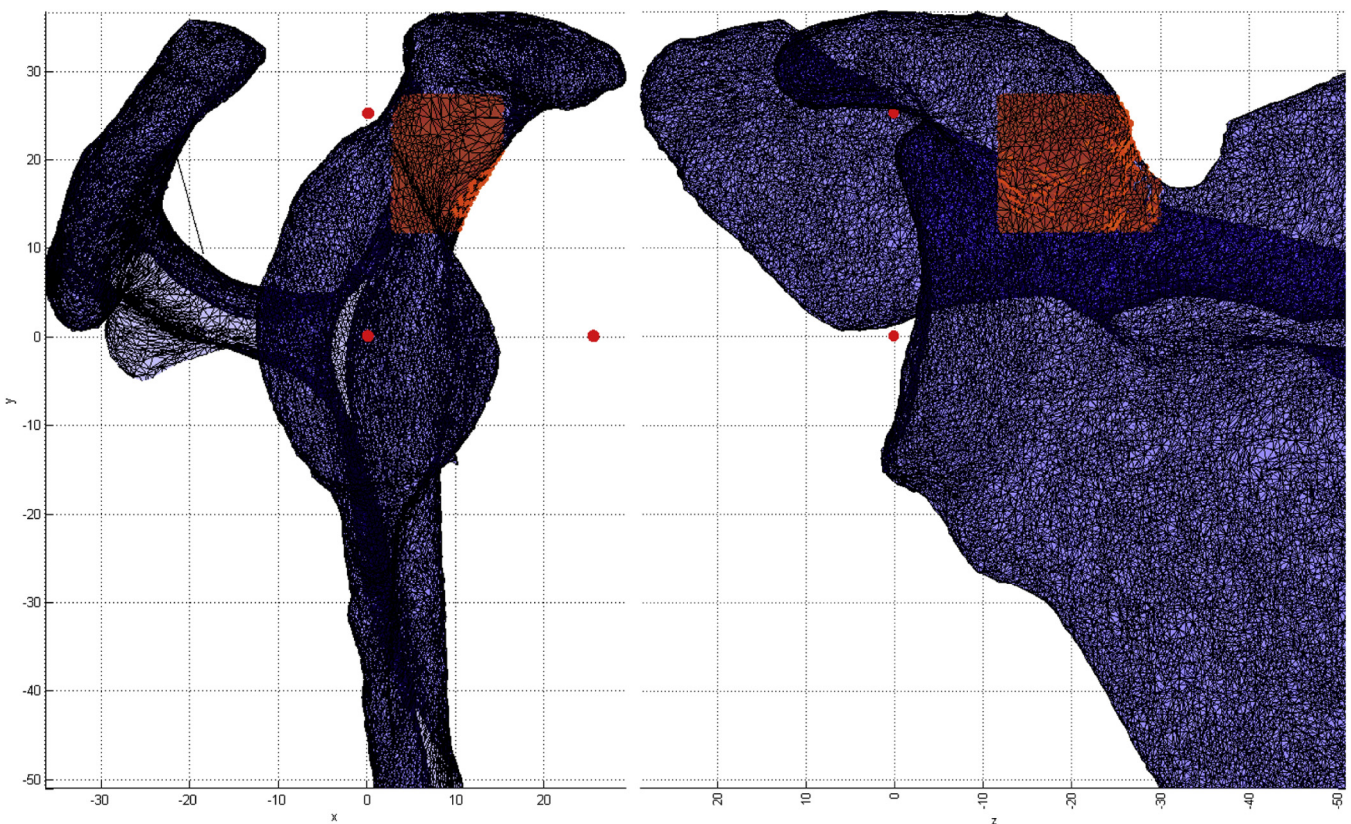


Figure 3 ROI in the superior coracoid region lateral to the suprascapular notch, as shown in the sagittal plane (Left) and coronal plane (Right). The 3 red dots represent the P1, P2, and P3 coordinate points from the assigned quadrupod. ROI, region of interest.

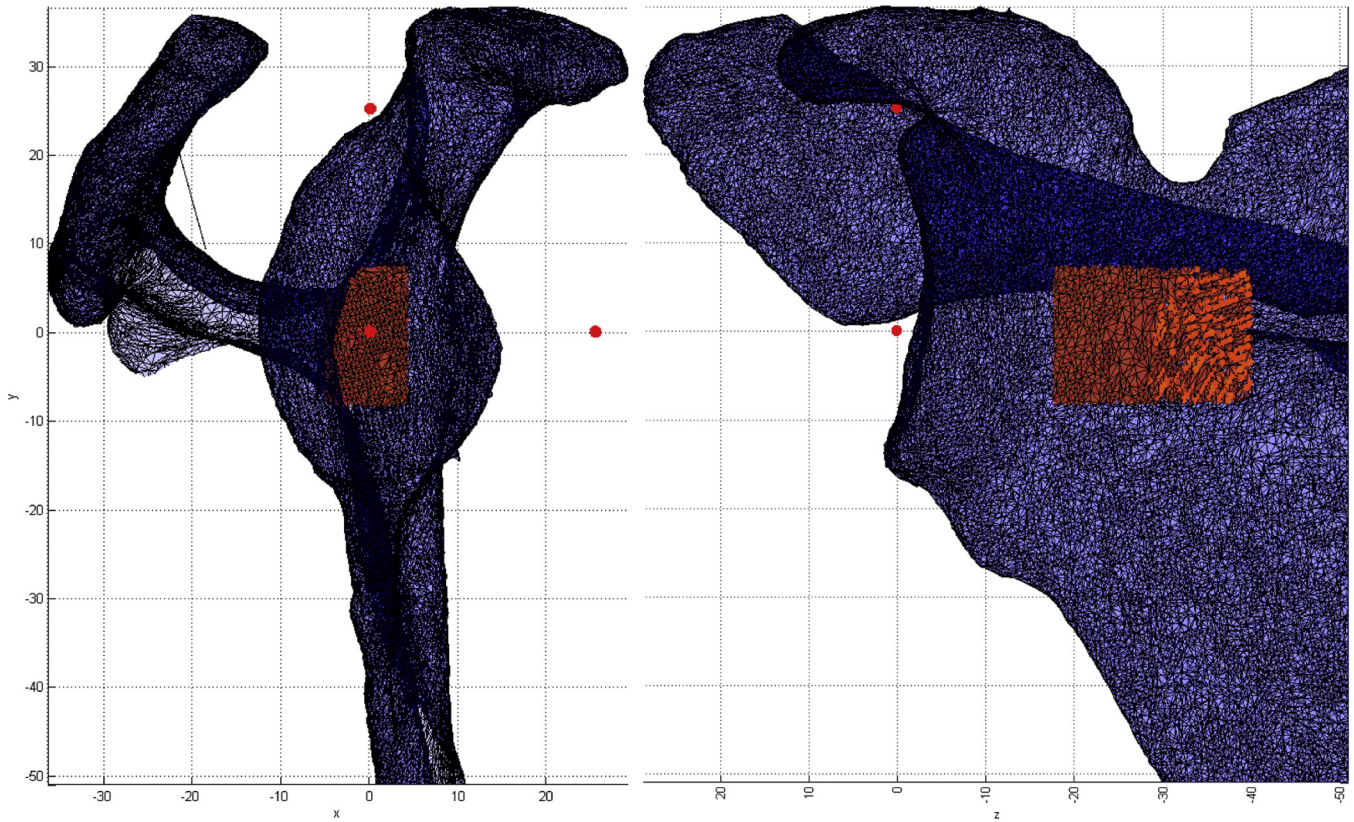


Figure 4 ROI in the anterior spine region, as shown in the sagittal plane (*Left*) and coronal plane (*Right*). The 3 red dots represent the P1, P2, and P3 coordinate points from the assigned quadripod. ROI, region of interest.

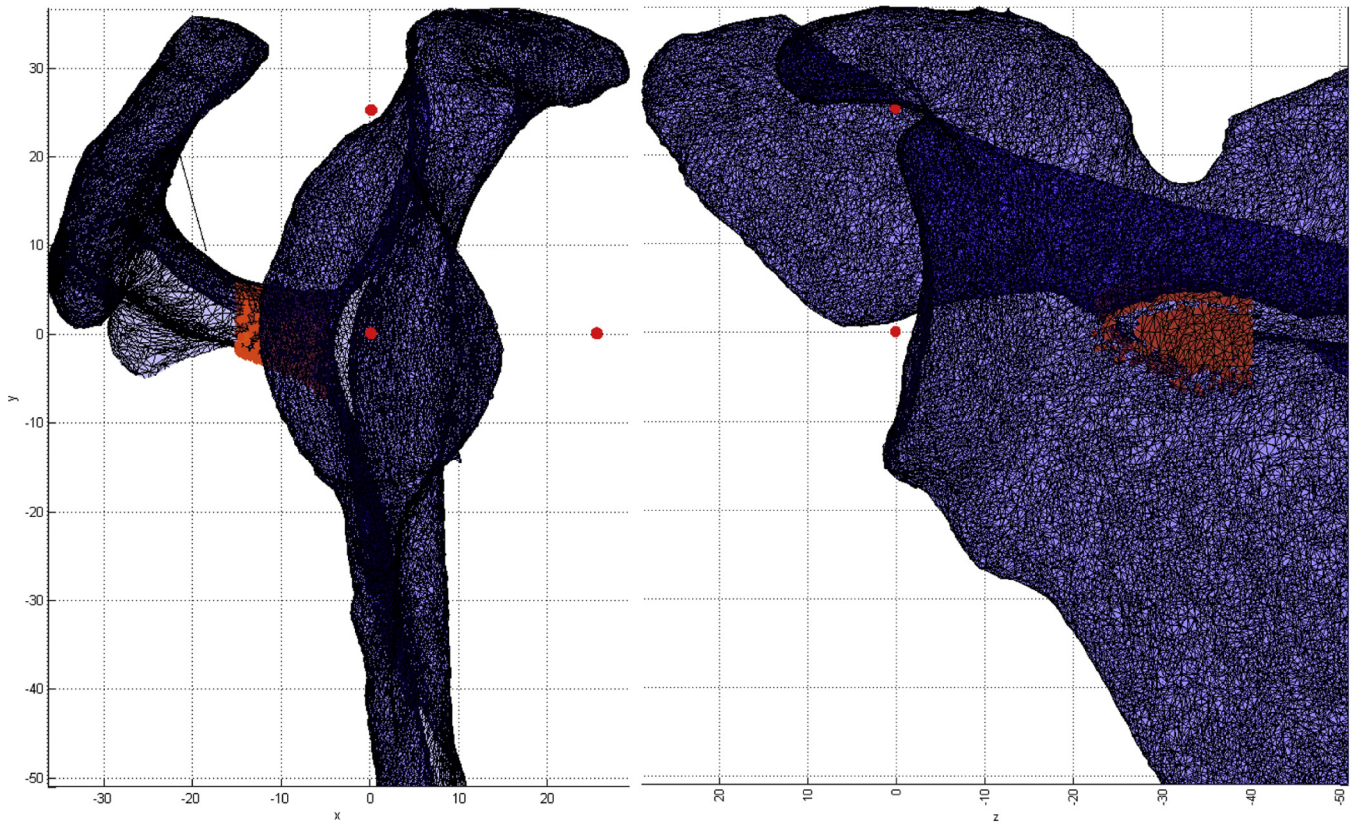


Figure 5 ROI in the posterior spine region, as shown in the sagittal plane (*Left*) and coronal plane (*Right*). The 3 red dots represent the P1, P2, and P3 coordinate points from the assigned quadripod. ROI, region of interest.

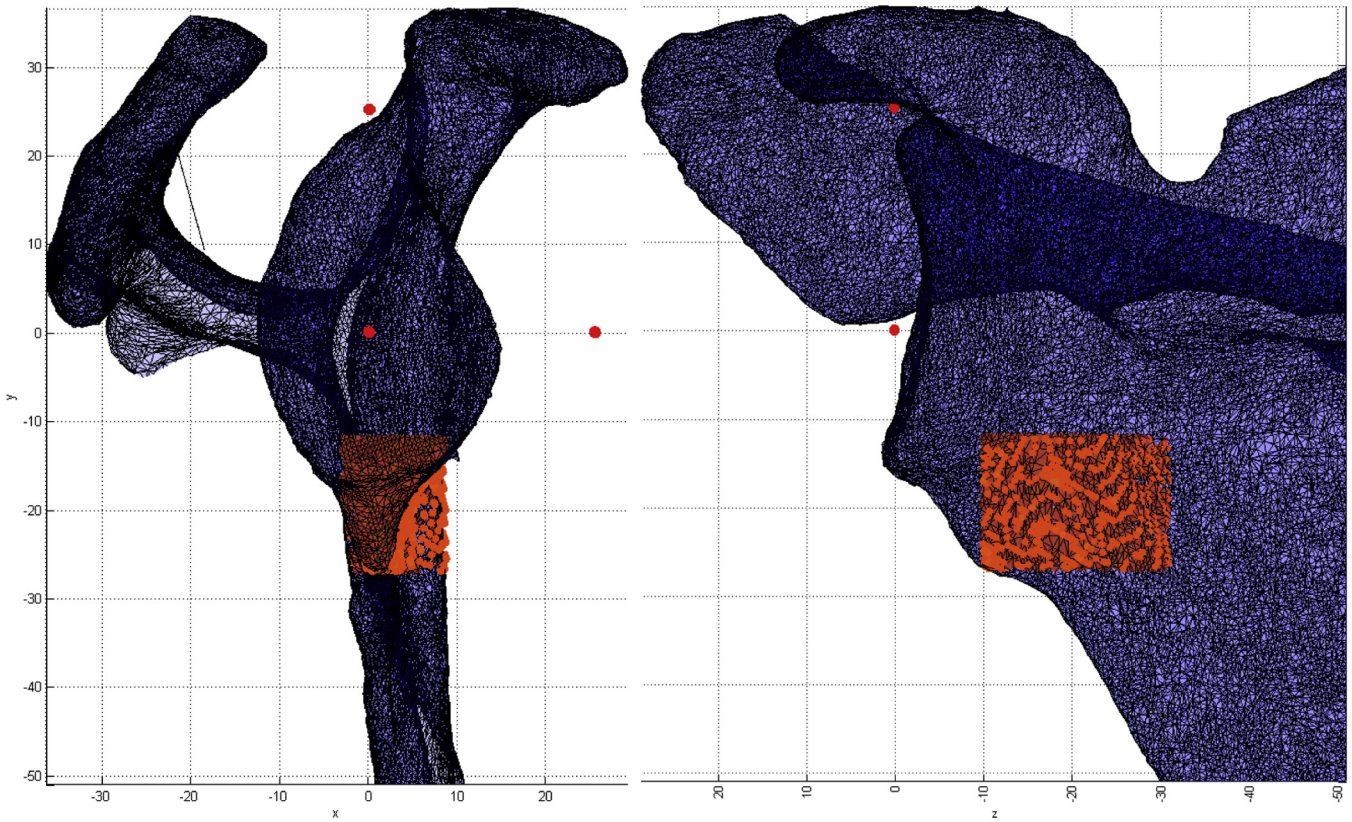


Figure 6 ROI in the anterosuperior lateral border region, as shown in the sagittal plane (*Left*) and coronal plane (*Right*). The 3 red dots represent the P1, P2, and P3 coordinate points from the assigned quadripod. ROI, region of interest.

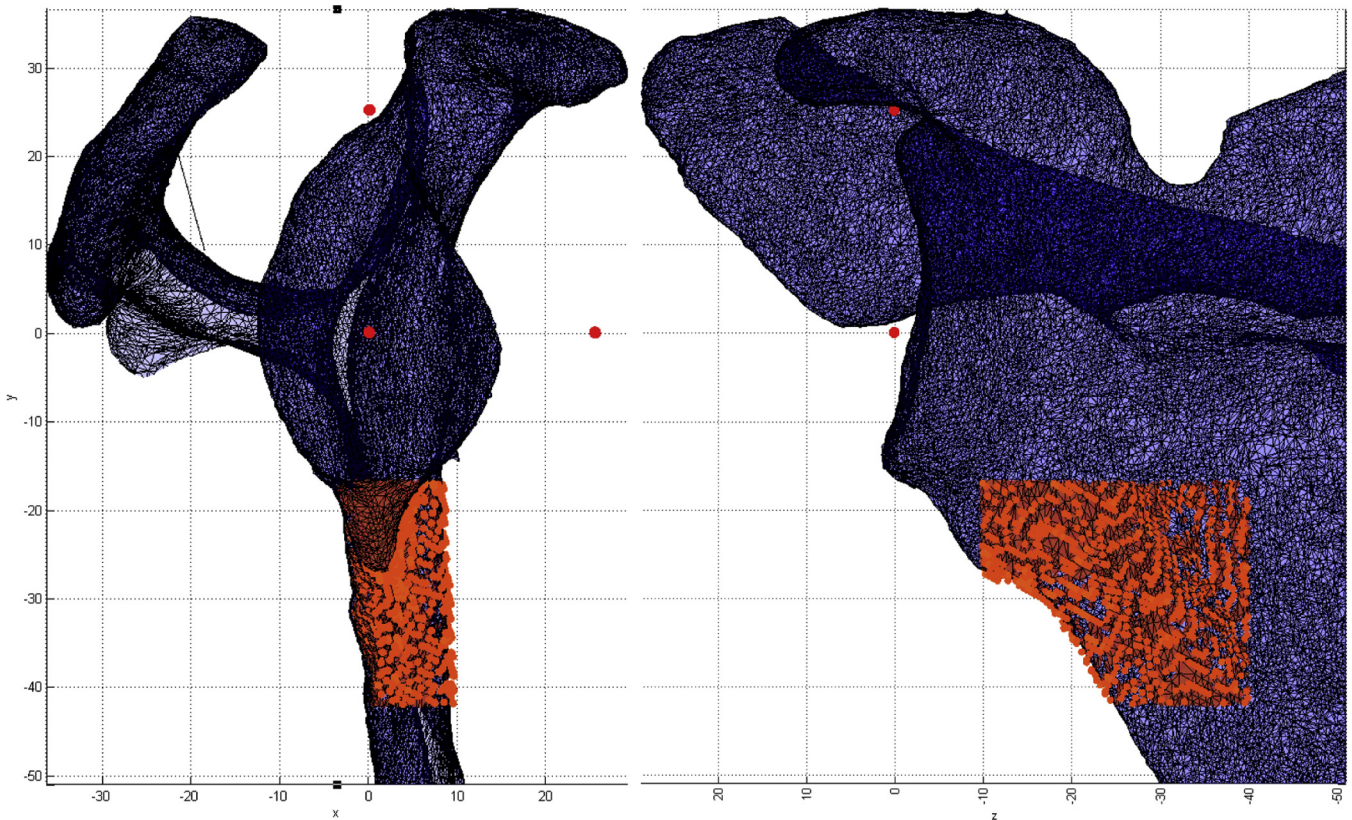


Figure 7 ROI in the inferior lateral border region, as shown in the sagittal plane (*Left*) and coronal plane (*Right*). The 3 red dots represent the P1, P2, and P3 coordinate points from the assigned quadripod. ROI, region of interest.

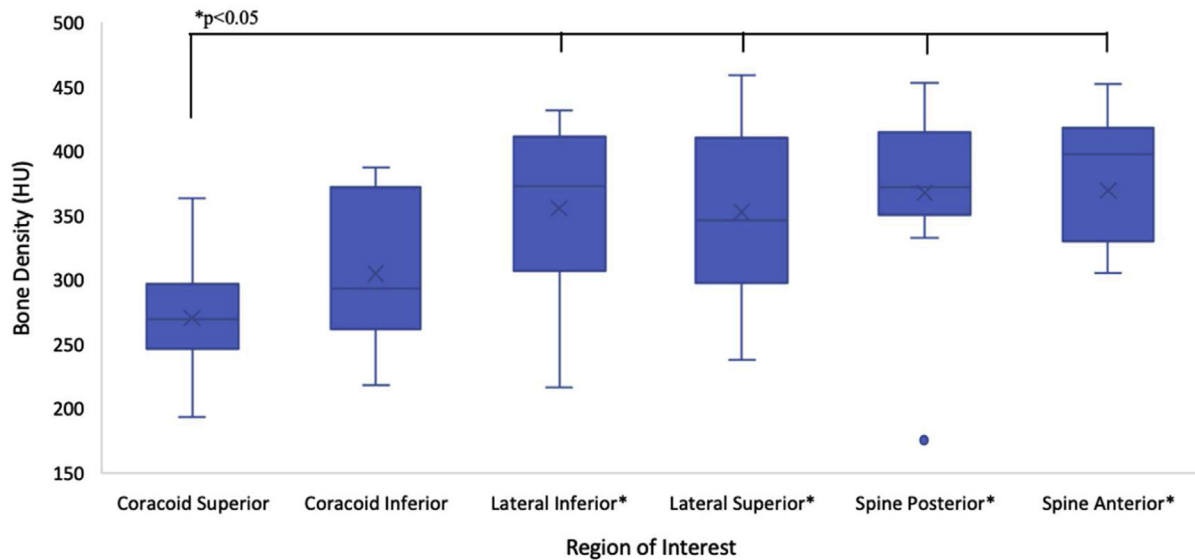


Figure 8 Trabecular bone density by region (n = 12).

chosen as the upper bound because it defines the cortico-cancellous interface in CT image data.^{1,13,24,29} Intraregion comparisons were performed on the anterior spine to the posterior portion of the scapular spine, the anterosuperior portion of the lateral border to the inferior portion of the lateral border, and the base of the coracoid inferior to the suprascapular notch compared with the base of the coracoid lateral to the suprascapular notch.

Statistical analyses

Inter-region comparisons were performed with the mean HU values of the coracoid, scapular spine, and lateral border ROIs. Statistical analysis utilized one-way analyses of variance with post hoc Bonferroni tests to compare the variance HU values and between the three columns of the scapula. An alpha value of 0.05 was considered statistically significant.

Results

The mean HU values of the ROI in the scapula ranged from 270 ± 45.6 HU to 370 ± 78.9 HU (Table 1). There were statistically significant inter-region differences between the mean HU values in the ROI (P < .05); however, there were no significant intraregion differences in trabecular bone density within each region of the coracoid (inferior and superior, P = 1.0), the lateral border (inferior and anterosuperior, P = 1.0), or the spine (between posterior and anterior, P = 1.0).

The box-and-whisker plot displays the mean HU value for each region of interest in the scapula (Fig. 8). The horizontal line in the middle of each box indicates the median, the top and bottom borders of the box mark the 75th and 25th percentiles, respectively, and the whiskers mark the 90th and 10th percentiles. *P < .05 indicates a region that is significantly different from the coracoid superior in the mean HU, wherein the coracoid’s inferior base is less dense than the spine and lateral border of the scapula.

We found that the coracoid superior lateral to the suprascapular notch was significantly less dense than the inferior portion of the lateral border (mean difference = 85.6 HU, P = .03, d_s = 1.54), anterosuperior portion of the lateral border (mean difference = 82.7 HU, P = .04, d_s = 1.42), posterior spine (mean difference = 97.6 HU, P = .007, d_s = 1.65), and anterior spine (mean

difference = 99.3 HU, P = .006, d_s = 1.54). There was no significant difference between the spine, lateral border, and coracoid inferior (P = 1.0).

Discussion

These results confirm that in vivo clinical CT scans on patients allow identification of ROIs with a higher bone density that may be suitable targets for screw placement during RSA. In addition, our results were comparable with those of our previous study that used higher-resolution CT scans of cadavers.⁹ We found that the coracoid superior region was significantly less dense than that of the ROIs in the spine and lateral border. This confirms our hypothesis that our results would be similar to those found by Daalder et al (2018), in which the lateral border and spine of the scapula contained denser bone than the base of the coracoid process. We also confirmed our hypothesis that there would be no differences in trabecular bone density within each anatomical region. Performing the previous analysis on patient scans is crucial as it demonstrates that our cadaveric results can be applied to actual patient care.

This study did not perform biomechanical testing on the scapula to determine if the results correlate with baseplate fixation or screw pullout strength. In addition, we analyzed only trabecular bone density distribution in the scapula and did not take into account the influence of surrounding cortical bone. However, the

Table 1 Average trabecular bone density by region (n = 12).

| Region | Bone density (HU) | | |
|----------------|-------------------|---------|---------|
| | Mean ± SD | Minimum | Maximum |
| Coracoid | | | |
| Superior | 270 ± 45.6* | 193 | 364 |
| Inferior | 305 ± 57.4 | 219 | 388 |
| Lateral border | | | |
| Anterosuperior | 353 ± 68.9* | 238 | 459 |
| Inferior | 356 ± 63.7* | 217 | 432 |
| Spine | | | |
| Anterior | 370 ± 78.9* | 171 | 453 |
| Posterior | 368 ± 70.0* | 176 | 453 |

HU, Hounsfield unit; SD, standard deviation.

*P < .05

literature demonstrates that screw purchase increases with greater trabecular bone density regardless of uncortical, bicortical, or cancellous only fixation.^{2,21,26} Previous studies have demonstrated that when a glenoid component is fixed to lesser dense bone, load failure is less,⁷ and as the stiffness of the surrounding bone where screws are inserted decreases, micromotion of the baseplate increases.¹⁵ Additional biomechanical studies need to be completed to validate the real-world application of this study's results.

Our findings provide important clinical applications. The intra-regional comparisons do not indicate differences in bone density within a subregion. Therefore, targeting screws to a specific area of the lateral border, spine, or coracoid process may not be necessary to achieve a greater trabecular bone purchase. When screw fixation is based only on the trabecular bone density affecting screw fixation, there is an increase in flexibility available to the surgeon when inserting variable angle screws in each location.

Concerning inter-region comparisons, our results suggest that less dense bone exists in the coracoid than in other areas of the scapula adjacent to the glenoid, which could provide useful information for glenoid baseplate redesign in RSA. Because studies have demonstrated that pullout strength decreases significantly as bone mineral density decreases, greater care should be taken when inserting a screw into the base of the coracoid so that it receives the best purchase in the bone.^{15,25}

DiStefano et al found that as long as other screws are not compromised, the best screw purchase is in the cortical bone at the base of the coracoid, in the inferior and slightly lateral margin of the suprascapular notch. Thus, surgeons have to strategically plan the trajectory of their screws into the base of the coracoid. This is because the coracoid has a small area of thick cortical bone available, compared with the lateral border and spine.

Although this study did not select ROIs based on a specific baseplate design, our future study will address this by analyzing regions in the traditional peripheral four-screw and central peg geometry. It is unknown if a variation of bone density exists as one shifts laterally to medially within each region. Understanding this could provide insight into varying screw or central peg lengths.

Finally, this study using patient data was comparable with that of our previous study in cadaveric specimens. Therefore, we can validate that our previous cadaveric results are applicable to *in vivo* clinical patients. Doing so demonstrates the applicability of our results in a patient setting, guiding future clinical studies to enable predictions regarding screw positioning during surgeries.

Conclusion

The coracoid was found to have significantly less dense trabecular bone than the ROIs in the spine or lateral border. Compared with the coracoid region, the higher density bone in the spine and lateral border may provide better bone purchase for screws when fixing the glenoid baseplate in RSA. These results hope to guide future studies surrounding RSA by enabling researchers to better integrate the anatomy of the scapulae when determining screw insertion trajectories and designing glenoid baseplates. These results were similar to what was found in our previous cadaveric study. Therefore, we can validate that our previous cadaveric results are applicable to *in vivo* clinical patients.

Disclaimers:

Funding: This study received no funding/grants.

Conflicts of interest: Ryan Bicknell receives financial payments for performing teaching and consulting activities for DePuy-Synthes Orthopaedics and Zimmer-Biomet Inc. The other authors, their immediate families, and any research foundation with which they

are affiliated have not received any financial payments or other benefits from any commercial entity related to the subject of this article.

Acknowledgments

The authors would like to acknowledge Heather Grant for her assistance with statistical analysis for this study.

References

1. Aamodt A, Kvistad KA, Andersen E, Lund-Larsen J, Eine J, Benum P, et al. Determination of the Hounsfield value for CT-based design of custom femoral stems. *J Bone Jt Surg* 1999;81:1-5.
2. Ab-Lazid R, Perilli E, John MK, Costi JJ, Reynolds KJ. Pullout strength of cancellous screws in human femoral heads depends on applied insertion torque, trabecular bone microarchitecture and areal bone mineral density. *J Mech Behav Biomed Mater* 2014;40:354-61. <https://doi.org/10.1016/j.jmbm.2014.09.009>.
3. Aggarwal A, Wahee P, Singh H, Aggarwal AK, Sahni D. Variable osseous anatomy of costal surface of scapula and its implications in relation to snapping scapula syndrome. *Surg Radiol Anat* 2011;33:135. <https://doi.org/10.1007/s00276-010-0723-4>.
4. Alentorn-Geli E, Samitier G, Torrens C, Wright TW. Review article reverse shoulder arthroplasty. Part 2: systematic review of reoperations, revisions, problems, and complications. *Int Shoulder Surg* 2015;9:60-7. <https://doi.org/10.4103/0973-6042.154771>.
5. Beckers A, Schenck C, Klesper B, Koebeke J. Comparative densitometric study of iliac crest and scapula bone in relation to osseous integrated dental implants in microvascular mandibular reconstruction. *J Craniomaxillofac Surg* 1998;26:75-83.
6. Burke CS, Roberts CS, Nyland JA, Radmacher PG, Acland RD, Voor MJ. Scapular thickness-implications for fracture fixation. *J Shoulder Elbow Surg* 2006;15:645-8. <https://doi.org/10.1016/j.jse.2005.10.005>.
7. Chebli C, Huber P, Watling J, Bertelsen A, Bicknell RT, Matsen F 3rd. Factors affecting fixation of the glenoid component of a reverse total shoulder prosthesis. *J Shoulder Elbow Surg* 2008;17:323-7. <https://doi.org/10.1016/j.jse.2007.07.015>.
8. Codsi MJ, Bennetts C, Powell K, Iannotti JP. Locations for screw fixation beyond the glenoid vault for fixation of glenoid implants into the scapula: an anatomic study. *J Shoulder Elbow Surg* 2007;16:S84-9. <https://doi.org/10.1016/j.jse.2006.07.009>.
9. Daalder MA, Venne G, Sharma V, Rainbow M, Bryant T, Bicknell RT. Trabecular bone density distribution in the scapula relevant to reverse shoulder arthroplasty. *J Shoulder Elbow Surg Int* 2018;2:174-81. <https://doi.org/10.1016/j.jses.2018.06.002>.
10. DeFranco MJ, Walch G. Current issues in reverse total shoulder arthroplasty. *J Musculoskelet Med* 2011;28:85-94.
11. DiStefano JG, Park AY, Nyugen TQ, Diecherichs G, Buckley JM, Montgomery WH. Optimal screw placement for base plate fixation in reverse total shoulder arthroplasty. *J Shoulder Elbow Surg* 2011;20:467-76. <https://doi.org/10.1016/j.jse.2010.06.001>.
12. Farshad M, Gerber C. Reverse total shoulder arthroplasty—from the most to the least common complication. *Int Orthop* 2010;34:1075-82. <https://doi.org/10.1007/s00264-010-1125-2>.
13. Fat DL, Galvin R, O'Brien F, McGrath F, Mullett H. The Hounsfield value for cortical bone geometry in the proximal humerus—an *in vitro* study. *Skeletal Radiol* 2012;41:557-68. <https://doi.org/10.1007/s00256-011-1255-7>.
14. Fevang BT, Lie SA, Havelin LI, Skredderstuen A, Furnes O. Risk factors for revision after shoulder arthroplasty. *Acta Orthop* 2009;80:83-91. <https://doi.org/10.1080/17453670902805098>.
15. Hitchon PW, Brenton MD, Coppes JK, From AM, Torner JC. Factors affecting the pullout strength of self-drilling and self-tapping anterior cervical screws. *Spine (Phila PA 1976)* 2003;28:9-13. <https://doi.org/10.1097/00007632-200301010-00004>.
16. Hopkins AR, Hansen UN, Bull MJ, Emery R, Amis A. Fixation of the reversed shoulder prosthesis. *J Shoulder Elbow Surg* 2008;17:974-80. <https://doi.org/10.1016/j.jse.2008.04.012>.
17. Humphrey CS, Kelly JD, Norris TR. Optimizing glenosphere position and fixation in reverse shoulder arthroplasty, part two: the three-column concept. *J Shoulder Elbow Surg* 2008;17:595-601. <https://doi.org/10.1016/j.jse.2008.05.038>.
18. James J, Allison MA, Werner FW, McBride DE, Basu N, Sutton CG, et al. Reverse shoulder arthroplasty glenoid fixation: is there a benefit in using four instead of two screws? *J Shoulder Elbow Surg* 2013;2:1030-6. <https://doi.org/10.1016/j.jse.2012.11.006>.
19. Karels A, Kegels L, De Wilde L. The pillars of the scapula. *Clin Anat* 2007;20:392-9. <https://doi.org/10.1002/ca.20420>.
20. Kelly JD, Humphrey CS, Norris TR. Optimizing glenosphere position and fixation in reverse shoulder arthroplasty, Part One: the twelve-mm rule. *J Shoulder Elbow Surg* 2008;17:589-94. <https://doi.org/10.1016/j.jse.2007.08.013>.

21. Lehtinen JT, Tingart MJ, Apreleva M, Warner JP. Quantitative morphology of the scapula: normal variation of the superomedial scapular angle and superior and inferior pole thickness. *Orthopedics* 2005;25:481-6. <https://doi.org/10.3928/0147-7447-20050501-15>.
22. Seebeck J, Goldhahn J, Städele H, Messmer P, Morlock MM, Schneider E. Effect of cortical thickness and cancellous bone density on the holding strength of internal fixator screws. *J Orthop Res* 2004;22:1237-42. <https://doi.org/10.1016/j.jorthres.2004.04.0>.
23. Stephens BF, Hebert CT, Azar FM, Mihalko WM, Throckmorton TW. Optimal baseplate rotational alignment for locking-screw fixation in reverse total shoulder arthroplasty: a three-dimensional computer-aided design study. *J Shoulder Elbow Surg* 2015;24:1367-71. <https://doi.org/10.1016/j.jse.2008.11.002>.
24. Teo JC, Si-Hoe KM, Keh JE, Teoh SH. Relationship between CT intensity, microarchitecture and mechanical properties of porcine vertebral cancellous bone. *Clin Biomech (Bristol, Avon)* 2006;21:235-44. <https://doi.org/10.1016/j.clinbiomech.2005.11.001>.
25. Tingart MJ, Lehtinen J, Zurakowski D, Warner JJ, Apreleva M. Proximal humeral fractures: regional differences in bone mineral density of the humeral head affect the fixation strength of cancellous screws. *J Shoulder Elbow Surg* 2006;15:620-4. <https://doi.org/10.1016/j.jse.2005.09.007>.
26. Vaughn DP, Syrcle JA, Ball JE, Elder SH, Gambino JM, Griffin RL, et al. Pullout strength of monocortical and bicortical screws in metaphyseal and diaphyseal regions of the canine humerus. *Vet Comp Orthop Traumatol* 2016;6:466-74. <https://doi.org/10.3415/VCOT-15-11-0192>.
27. Venne G, Pickell M, Pichora DR, Bicknell RT, Ellis RE. CT image registration for evaluating reverse shoulder arthroplasty placement. *Orthopaedic Proc* 2018;96.
28. von Schroder HP, Kuper SD, Botte MJ. Osseous anatomy of the scapula. *Clin Orthop Relat Res* 2001;383:131-9.
29. Wiest S, Maillot C, Koritke JG. Dimensions of the human scapula. *Arch Anat Histol Embryol* 1985;68:127-37.